INVESTIGATIONS OF ELECTRONIC INTERACTIONS BETWEEN *closo*-BORANES AND TRIPLE-BONDED SUBSTITUENTS

Piotr KASZYNSKI[a1,*], Serhii PAKHOMOV[a2] and Victor G. YOUNG, Jr.[b]

[a] *Organic Materials Research Group, Department of Chemistry, Vanderbilt University, Nashville, TN 37235, U.S.A.; e-mail: [1] piotr@ctrvax.vanderbilt.edu, [2] serhii@lsu.edu*

[b] *X-Ray Crystallographic Laboratory, Department of Chemistry, University of Minnesota, Twin Cities, MN 55455, U.S.A.; e-mail: young@chemsun.chem.umn.edu*

Received May 2, 2002
Accepted June 24, 2002

Dedicated to Professor Jaromír Plešek on the occasion of his 75th birthday.

Intramolecular electronic interactions were investigated in five series of 12-, 10-, and 6-vertex *closo*-boranes and hydrocarbons (benzene, acetylene, bicyclo[2.2.2]octane, and cubane) substituted with triple-bonded groups Y≡Z (C≡CR, C≡N, C≡O, and N≡N). Structural data (single crystal X-ray crystallography), spectroscopic properties (UV, IR, and NMR), chemical behavior (dediazoniation reactions), and electronic structure calculations (hybridization and π bond order) are all in agreement that the degree of electronic conjugation between the cluster and the Y≡Z substituent is lowest for the 12-vertex *closo*-borane and highest for the 6-vertex analog.

Keywords: Carboranes; Boranes; Structure elucidation; *Ab initio* calculations; π Interactions; Electron transmission; X-ray diffraction; Substituent effects.

The geometrical and electronic properties of *closo*-boranes continue to attract attention in the context of design and construction of molecular and supramolecular materials. Of particular interest are electronic interactions between 12-vertex (**1**), 10-vertex (**2**) and 6-vertex (**3**) clusters and π substituents and through-cage electron transmission effects (Fig. 1).

closo-Boranes are considered to be three-dimensional aromatic species[1], possessing a set of molecular orbitals with π symmetry[2]. For this reason, there has been a substantial effort to study electronic interactions in derivatives of the 12-vertex[3] and, to a lesser extent, 10-vertex clusters. Other clusters, including the 6-vertex *closo*-borane, received very little attention in this context[4]. Early studies established that 12-vertex *p*-carborane has a small positive Hammett sigma value (σ_p = +0.14), which was ascribed solely to the inductive effect[3,5]. Similar studies for the 10-vertex carborane gave a

Hammett value of σ_p = +0.05 (ref.[6]). Spectroscopic studies demonstrated a rather moderate effect of the 12-vertex *closo*-borane on aromatic substituents[5,7,8]. Only in the case of inner salts of 12-vertex *closo*-borates substituted with a tropylium ion, a strong charge-transfer band[9,10] and a significant first hyperpolarizability β were observed[10]. In contrast, experiments demonstrated that 12-vertex carborane is completely ineffective as a structural element of NLO materials[7,11]. Recent calculations showed, however, that when substituted with a powerful donor and acceptor, 12-vertex acts as an electron conduit[12]. Another recent study of the electron transmission properties of 12-vertex *p*-carborane were inconclusive, but suggested that the iron centers are weakly coupled at best[13].

The few studies concerning the 10-vertex *closo*-boranes showed significantly stronger electronic interactions between the cluster and π substituents that those observed in the 12-vertex analogs. This is evident from intense and relatively low energy absorption bands observed for aryl[14–16], azo[17,18], diazo[14] and other[19,20] derivatives of 10-vertex boranes. Limited data for 6-vertex cluster derivatives suggest similar strong electronic interactions[21].

Several years ago we began a concerted effort to better understand the extent of such electronic interactions in the context of designing molecular materials with controllable electronic and photophysical properties[22–24].

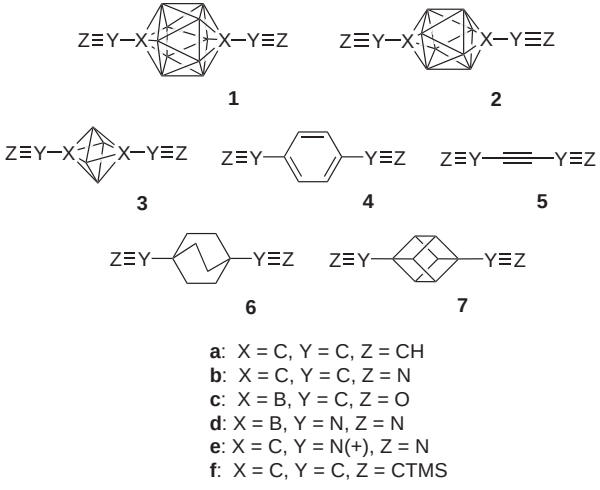

FIG. 1

Derivatives of 12-, 10-, and 6-vertex *closo*-boranes (**1**, **2**, and **3**, respectively), benzene (**4**), acetylene (**5**), bicyclo[2.2.2]octane (**6**) and cubane (**7**). In structures **1**–**3** each unsubstituted vertex corresponds to a BH fragment

Our studies have shown that aryl derivatives of the 10-vertex cluster exhibit strong absorption bands of lower energy than those in the corresponding 12-vertex analogs[25]. Calculations also suggest that 10-vertex and 6-vertex clusters are significantly more effective structural elements for NLO materials than 12-vertex boranes[25]. A full account of these results will be presented elsewhere. In this paper we focus on triple-bonded substituents. Specifically, we consider *closo*-boranes symmetrically disubstituted in the antipodal positions (Fig. 1), which are readily experimentally available. We recently reported that dinitrile and diacetylene derivatives of 10-vertex carborane, **2b** and **2f**, exhibit electronic absorption bands similar to those in benzene analogs[24]. In other studies, we discussed structural and spectroscopic properties of acetylene derivatives of 10- and 12-vertex carboranes[26]. To our knowledge, the bonding between the clusters and the Y≡Z substituent has been discussed only for **1c** [27,28] and **2d** [29], and, aside from our limited studies[24,25], no systematic comparison has appeared.

Here we report the synthesis, and molecular and electronic structures of two derivatives of 1,12-dicarba-*closo*-dodecaborane, diacetylene **1f**, a simple derivative of **1a**, and dinitrile **1b**. We provide an extensive analysis and comparison of bonding between 12-, 10- and 6-vertex boron clusters and triple-bonded substituents C≡CR, C≡N, C≡O and N≡N. The results for the clusters are compared with those for analogs of three hydrocarbon benchmarks: benzene (**4**), acetylene (**5**), and bicyclo[2.2.2]octane (**6**). We also include cubane analogs (**7**) in the comparison because the hybridization of the carbon exocyclic bond is similar to that in benzene. Finally, we discuss the relative magnitude of electronic interactions in the clusters and hydrocarbons and its manifestation in structural, chemical, and spectroscopic properties.

RESULTS AND DISCUSSION

Synthesis

Diacetylene **1f** was prepared from 1,12-dicopper-1,12-dicarba-*closo*-dodecaborane and 1-bromo-2-trimethylsilylacetylene according to a modified literature procedure[30,31]. Dinitrile **1b** was obtained by dehydration of 1,12-dicarba-*closo*-dodecaborane-1,12-dicarboxamide (**8**) with poly(trimethylsilyl phosphate) using a general procedure[32] (Scheme 1).

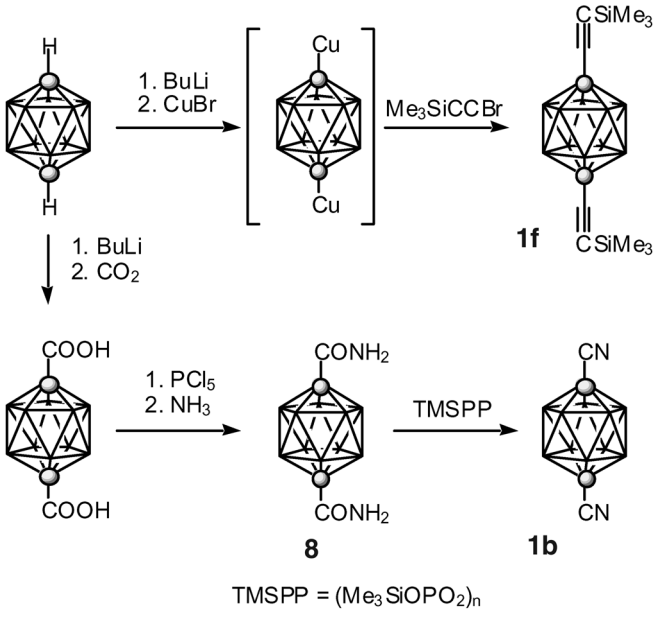

SCHEME 1

Molecular and Crystal Structures

Colorless crystals of compounds were obtained by slow sublimation under atmospheric (**1b**) or reduced pressure (**1f**), and their solid state structures were determined by X-ray analysis. The experimental details are presented in Table I, and selected bond lengths and angles for the two compounds are shown in Tables II and III.

The molecules of silane **1f** shown in Fig. 2 lie on an inversion center. The C≡C distance is 1.193(3) Å and is longer than that reported for the parent diacetylene **1a** (1.180(3) Å)[31]. This presumably reflects the influence of the

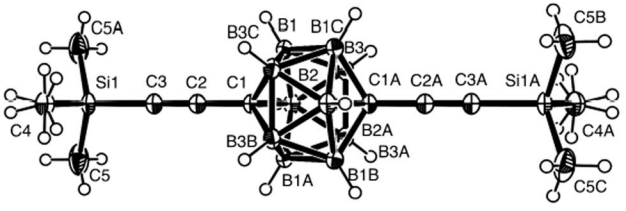

FIG. 2
Thermal ellipsoid diagram of 1,12-bis[(trimethylsilyl)ethynyl]-1,12-dicarba-*closo*-dodecaborane (**1f**) drawn at 50% probability. Selected molecular dimensions are listed in Table II

electron-donating silicon substituent. Other molecular dimensions are very close to those reported for **1a** [31] and are well reproduced by *ab initio* calculations (Table II).

In the dinitrile **1b** shown in Fig. 3, the average C≡N and C–C bond lengths for two independent molecules are 1.1433(18) and 1.452(18) Å. The calculated (HF/6-31G*) C–C distance of 1.451 Å compares well to the experimental value, while the C≡N distance is predicted to be about 0.01 Å shorter than the observed value (Table III). The presence of the strong electron withdrawing CN substituent has a noticeable effect on the cage geometry. The C···C distance in **1b** (3.056 Å) is shorter than that found in **1a** (3.104(2) Å)[31] and similar to that reported for parent *p*-carborane (3.056(4) Å [33] and 3.05 Å [34]). At the same time, the B–C distance in **1a** and **1b** (1.726(3) and 1.720(2) Å) is significantly longer than that in the parent *p*-carborane (1.704(5) Å [33] and 1.710(11) Å [34]). These trends are well repro-

TABLE I
Crystallographic data[a]

Parameter	**1f**	**1b**
Chemical formula	$C_{12}H_{28}B_{10}Si_2$	$C_4H_{10}B_{10}N_2$
Formula weight	336.62	194.24
Space group	*C*2/*m*	$P\bar{1}$
a, Å	21.739(3)	7.108(1)
b, Å	7.5588(9)	7.401(1)
c Å	7.0071(8)	10.766(2)
α, °	90	82.554(3)
β, °	107.836(2)	75.372(3)
γ, °	90	77.139(3)
V, Å^3	1096.1(2)	532.6(2)
Z	2	2
D_{calc}, g/cm^3	1.020	1.211
μ, mm^{-1}	0.154	0.059
R^b (observed)	0.0407	0.0436
$R_w{}^c$ (observed)	0.1117	0.1181

[a] Temperature 173(2) K and λ = 0.71073 Å. [b] $R = \Sigma||F_o| - |F_c||/\Sigma |F_o|$. [c] $R_w = \{\Sigma[w(F_o^2 - F_c^2)^2]/\Sigma[w(F_o^2)^2]\}^{1/2}$.

TABLE II
A comparison of selected values of bond distances (in Å) and angles (in °) for **1f** with diacetylene **1a** experimental and calculated values

Atoms	**1f**	**1a**	
		experimental[a]	calculated[b]
C(3)–Si(1)	1.857(2)	–	–
C(3)–C(2)	1.193(3)	1.180(3)	1.185
C(2)–C(1)	1.452(2)	1.451(2)	1.449
C(1)–B (average)	1.726(2)	1.726(3)	1.723
B–B belt (average)	1.789(2)	1.793(3)	1.796
B–B inter-belt (average)	1.765(2)	1.761(3)	1.769
C(1)–C(2)–C(3)	179.1(2)	179.18	180
B–C(1)–C(2) (average)	118.15(15)	117.91	117.55
B–B–C(1) (average)	104.71(12)	104.86	104.18
C–B–B–C (average)	59.77(14)	59.61	59.16

[a] Average values for two independent molecules: ref.[31]. [b] The HF/6-31G* level of theory.

TABLE III
Selected average bond distances (in Å) and angles (in °) for two independent molecules of dinitrile **1b** in the unit cell

Atoms	Molecule I	Molecule II	Calculated[a]
C–N	1.1442(18)	1.1423(19)	1.134
C–C	1.4546(19)	1.4505(19)	1.451
C–B (average)	1.720(2)	1.719(2)	1.722
B–B belt (average)	1.797(2)	1.799(2)	1.804
B–B inter-belt (average)	1.758(2)	1.760(2)	1.768
N–C–C (average)	178.18(15)	179.29(15)	180
C–C–B (average)	117.28(11)	117.12(11)	117.00
C–B–B (average)	103.83(11)	103.69(11)	103.62
C–B–B–C (average)	58.89(13)	58.98(13)	58.69

[a] The HF/6-31G* level of theory.

duced by ab initio calculations, and are consistent with computational results[35] for 12 disubstituted *p*-carboranes, including **1b**, obtained at the MP2 level of theory.

*Comparison of **1** with Other Clusters*

A comparison of **1f** with the 10-vertex analog shows that the C–C bond is longer and the C≡C distance is shorter in **1f** than in **2f** (Table IV). Similarly, the experimental C–C and C≡N distances are longer and shorter, respectively, in the 12-vertex dinitrile **1b** than in the 10-vertex analog **2b** (Table V). Although these differences are crystallographically insignificant (within 3σ), the trend is well reproduced computationally, and appears to be general for all derivatives **1** and **2** (Tables IV–VIII). Computational results show that the observed distortion of the X–Y≡Z bonds towards the allene-type structure X=Y=Z is even more pronounced in the 6-vertex derivatives **3**.

The calculated and experimental X–Y distances in boron clusters **1**–**3** fall in a middle range between those found in bicyclo[2.2.2]octane[36–38] (**6**) and acetylene[39,40] (**5**) derivatives and are generally close to those found in benzene[41–43] (**4**) and cubane[44] (**7**). For instance, the calculated C–CN distances for carborane nitriles **1b**–**3b** are between 1.452 and 1.435 Å which is approximately in the middle of a range defined by the longest and the shortest C–CN distances among the nitriles found in **6b** (calculated 1.476 Å, experimental[38] 1.471(4) Å) and dicyanoacetylene, **5b** (calculated 1.390 Å, experimental[40] 1.37 Å), respectively. A similar trend is observed in the acetylene derivatives and also in the bisdiazonium cations. In the latter series (Table VIII), the C–NN distances in the carborane, benzene and cubane de-

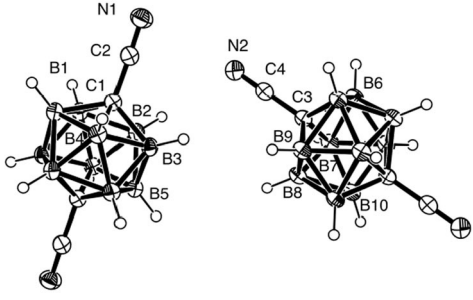

FIG. 3
Thermal ellipsoid diagram of 1,12-dicarba-*closo*-dodecaborane-1,12-dicarbonitrile (**1b**) drawn at 50% probability. Selected molecular dimensions are listed in Table III

rivatives are about 1.43 Å and fall in the middle range between extremes defined by **6e** (1.570 Å) and **5e** (1.340 Å).

The results suggest that the tendency towards the "allenic distortion" is consistent in all series of compounds and increasing in the following order: 12-vertex < 10-vertex < 6-vertex.

Analysis of the structural data in Tables IV–VIII shows excellent agreement between calculated and experimental values for the X–Y≡Z groups. The overall correlation is high (R^2 = 0.994) with std for the calculated differences of 0.013 Å. The largest deviation from the experiment (0.027 Å) is observed for **5a** and can be ascribed to the low precision of the experiment[40].

TABLE IV
Comparison of bonding in diacetylenes (HC≡C–A–C≡CH)

Compound	A	Bond length[a]		Hybridization[b]		π Bond order[c]	
		C–C	C≡C	C_{cage}–	–C≡	C–C	C≡C
1a	1,12-$C_2B_{10}H_{10}$	1.4493 1.452(2)[d] 1.451(2)[e]	1.1847 1.193(2)[d] 1.180(3)[e]	$sp^{2.26}$	$sp^{1.18}$	0.055	1.936
2a	1,10-$C_2B_8H_8$	1.4390 1.436(2)[f]	1.1853 1.199(2)[f]	$sp^{2.17}$	$sp^{1.17}$	0.058	1.935
3a	1,6-$C_2B_4H_4$	1.4325	1.1858	$sp^{1.85}$	$sp^{1.16}$	0.067	1.928
4a	1,4-C_6H_4	1.4414 1.444[g]	1.1881 1.188[g]	$sp^{2.30}$	$sp^{1.14}$	0.069	1.929
5a	1,2-C≡C	1.3848 1.375(16)[h]	1.1880 1.199(17)[h]	$sp^{1.15}$	$sp^{1.19}$	0.115	1.883
6a	1,4-BCO	1.4739 1.468[i]	1.1877 1.189[i] 1.187[j]	$sp^{2.97}$	$sp^{1.12}$	0.036	1.960
7a	1,4-cubane	1.4465 1.438[k]	1.1885 1.181[k]	$sp^{2.15}$	$sp^{1.14}$	0.054	1.944

[a] The HF/6-31G* level of theory. [b] The exo-cage bond hybrid obtained from NBO 3.1. [c] MNDO//HF/6-31G* calculations. [d] Experimental value for the trimethylsilyl derivative **1f**: This work. [e] Average value for two independent molecules: ref.[31]. [f] Average experimental value for the trimethylsilyl derivative **2f**: ref.[24]. [g] Ref.[41]. [h] Experimental value for the dimethyl derivative (Z = C–Me): ref.[39]. [i] Experimental value for a diaryl derivative (Z = C–Ar): ref.[36]. [j] Found in a terminal alkyne: ref.[37]. [k] Average value for two independent molecules: ref.[44]

TABLE V
Comparison of bonding in dinitriles (N≡C–A–C≡N)

Compound	A	Bond length[a]		Hybridization[b]		π Bond order[c]	
		C–C	C≡N	C_{cage}–	–C≡	C–C	C≡N
1b	1,12-$C_2B_{10}H_{10}$	1.4515 1.453(2)[d]	1.1338 1.143(2)[d]	$sp^{2.55}$	$sp^{0.93}$	0.042	1.950
2b	1,10-$C_2B_8H_8$	1.4403 1.438(2)[e]	1.1342 1.146(2)[e]	$sp^{2.42}$	$sp^{0.93}$	0.045	1.946
3b	1,6-$C_2B_4H_4$	1.4349	1.1344	$sp^{2.03}$	$sp^{0.93}$	0.051	1.942
4b	1,4-C_6H_4	1.4454 1.441(2)[f]	1.1358 1.133(2)[f]	$sp^{2.49}$	$sp^{0.91}$	0.052	1.939
5b	1,2-C≡C	1.3895 1.37[g]	1.1357 1.14[g]	$sp^{1.19}$	$sp^{0.98}$	0.084	1.911
6b	1,4-BCO	1.4759 1.471(4)[h]	1.1355 1.133(4)[h]	$sp^{3.24}$	$sp^{0.88}$	0.031	1.957
7b	1,4-cubane	1.4483	1.1363	$sp^{2.33}$	$sp^{0.91}$	0.044	1.946

[a] The HF/6-31G* level of theory. [b] The exo-cage bond hybrid obtained from NBO 3.1. [c] MNDO//HF/6-31G* calculations. [d] Average experimental value for two independent molecules: This work. [e] Ref.[24]. [f] Ref.[42]. [g] Ref.[40]. [h] Experimental value for 1,4-dicyanocyclohexane: ref.[38]

TABLE VI
Comparison of bonding in diacarbonyl derivatives (O≡C–A–C≡O)

Compound	A	Bond length[a]		Hybridization[b]		π Bond order[c]	
		B–C	C≡O	B–	–C≡	B–C	C≡O
1c	1,12-$B_{12}H_{10}$	1.5678 1.543(2)[d]	1.1049 1.119(2)[d]	$sp^{5.93}$	$sp^{0.52}$	0.072	1.540
2c	1,10-$B_{10}H_8$	1.5254	1.1082	$sp^{2.67}$	$sp^{0.53}$	0.109	1.490
3c	1,6-B_6H_4	1.5285	1.1094	$sp^{2.62}$	$sp^{0.53}$	0.118	1.470
	C≡O	–	1.1138	–	–	–	1.542

[a] The HF/6-31G* level of theory. [b] The exo-cage bond hybrid obtained from NBO 3.1. [c] MNDO//HF/6-31G* calculations. [d] Ref.[28]

Other significant differences are observed for the carbonyl and diazo derivatives **1c** and **2d**. With those removed from the correlation, the R^2 factor increases to 0.997, and the standard deviation for the difference is 0.009 Å.

TABLE VII
Comparison of bonding in bisdiazo derivatives (N≡N–A–N≡N)

Compound	A	Bond length[a]		Hybridization[b]		π Bond order[c]	
		B–N	N≡N	B–	–N≡	B–N	N≡N
1d	1,12-$B_{12}H_{10}$	1.5808	1.0740	$sp^{7.07}$	$sp^{0.64}$	0.049	1.926
2d	1,10-$B_{10}H_8$	1.5241 1.499(2)[d]	1.0757 1.091(2)[d]	$sp^{1.01}$	$sp^{1.33}$	0.079	1.886
3d	1,6-B_6H_4	1.5219	1.0767	$sp^{2.10}$	$sp^{1.30}$	0.088	1.873
	N≡N	–	1.0784	–	–	–	2.000

[a] The HF/6-31G* level of theory. [b] The exo-cage bond hybrid obtained from NBO 3.1. [c] MNDO//HF/6-31G* calculations. [d] Ref.[29]

TABLE VIII
Comparison of bonding in bisdiazo dication derivatives ($(N≡N–A–N≡N)^{2+}$)

Compound	A	Bond length[a]		Hybridization[b]		π Bond order[c]	
		C–N	N≡N	C_{cage}–	–N≡	C–N	N≡N
1e	1,12-$C_2B_{10}H_{10}$	1.4455	1.0743	$sp^{5.01}$	$sp^{0.83}$	0.049	1.892
2e	1,10-$C_2B_8H_8$	1.4216	1.0743	$sp^{4.46}$	$sp^{0.84}$	0.056	1.886
3e	1,6-$C_2B_4H_4$	1.4106	1.0750	$sp^{3.44}$	$sp^{0.86}$	0.061	1.877
4e	1,4-C_6H_4	1.4391 1.416(4)[d]	1.0756 1.086(3)[d]	$sp^{3.86}$	$sp^{0.85}$	0.062	1.882
5e	1,2-C≡C	1.3397	1.0799	$sp^{1.50}$	$sp^{0.97}$	0.115	1.809
6e	1,4-BCO	1.5695	1.0742	$sp^{6.79}$	$sp^{0.80}$	0.021	1.932
7e	1,4-cubane	1.4498	1.0753	$sp^{3.80}$	$sp^{0.84}$	0.052	1.896
	N≡N	–	1.0784	–	–	–	2.000

[a] The HF/6-31G* level of theory. [b] The exo-cage bond hybrid obtained from NBO 3.1. [c] MNDO//HF/6-31G* calculations. [d] Values for 4-nitrobenzenediazonium salt: ref.[43]

Hybridization and π Bond Order

Results from Natural Bond Order analyses provide insight into hybridization of the X–Y≡Z atoms. The s-character of the exocyclic bond to the substituent formed by the apical atoms X in boron clusters appears to be generally highest in the 6-vertex derivatives and lowest in the 12-vertex derivatives. For instance, the apical carbon in the 6-vertex derivative **3a** uses a $sp^{1.85}$ hybridized orbital to bond to the substituent, while in the 12-vertex analog **1a** the same orbital is $sp^{2.26}$ hybridized. These values are comparable to those calculated for benzene and cubane ($sp^{2.30}$ for **4a** and $sp^{2.15}$ for **7a**), and are approximately in the middle of a range defined by bicyclo[2.2.2]octane **6a** ($sp^{2.97}$) and acetylene **5a** ($sp^{1.15}$). The highest contribution of the s orbital to the bond hybrid is observed in the acetylenes, lower in the nitriles, and lowest in the diazo derivatives. An exception from these trends is observed in the neutral bisdiazo derivatives **1d**–**3d**. The bond of the apical boron atom to the N_2 group in 10-vertex derivative **2d** has a much higher s-character ($sp^{1.01}$) than that in the 6-vertex analog ($sp^{2.10}$). It is also noticeable that the orbital forming the exocyclic bond in 12-vertex carbonyl and diazo derivatives has almost pure p-character (*e.g.* $sp^{7.07}$ in **1d** and $sp^{5.01}$ in **1e**), which parallels the calculated hybrid for bicyclo[2.2.2]octane derivative **6e** ($sp^{6.79}$). This, combined with the long X–Y bonds and low dediazoniation energy, suggests a loose character of the bond.

Analysis of bond order and especially the π component for the X–Y≡Z fragment is useful for better understanding of the electronic interactions between the ring and the substituent[45]. Trends in π bond orders in the series of compounds parallel those in hybridization as shown for the acetylenes in Fig. 4. The highest π bond order of the C–C bond is calculated for acetylene derivatives **5** (*e.g.* 0.115 for **5a**) and the smallest for bicyclo[2.2.2]octane compounds **6** (*e.g.* 0.036 for **6a**). The values for clusters **1**–**3** fall in the middle of this range, and those for the 6-vertex cluster are largest among the three boranes. The overall correlation factor R^2 in Fig. 4 is only 0.86. It appears however, that good correlation exists for three boranes **1a**–**3a** (R^2 = 0.999), and also for hydrocarbons excluding cubane **7** (R^2 = 0.997). Exceptionally large π bond orders are observed for B–C bonds in the carbonyl derivatives in which the value of 0.118 has been calculated for the 6-vertex derivative **3d**.

With the increasing π bond order for the X–Y bond, the Y≡Z is proportionally depopulated. This is consistent with the "allenic distortion" of the triple-bonded substituent.

The observed and calculated interatomic distances reflect the electronic properties of the bonds. Not surprisingly, the hybridization and bond order correlate well with the X–Y distances graphically presented for the nitriles in Fig. 5.

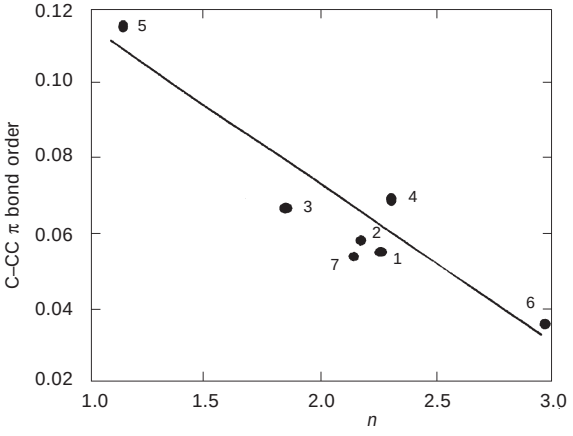

FIG. 4
Correlation between hybridization (*n* is the exponent in sp^n) of the ring carbon atom exocyclic bond and the C–C≡C π bond order in acetylenes

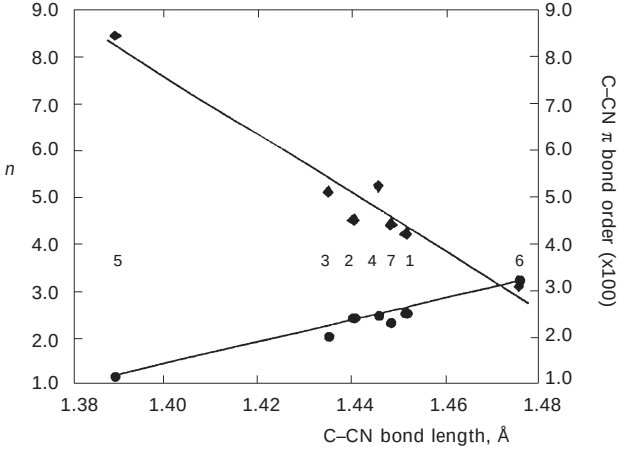

FIG. 5
Correlation between C–CN bond length and hybridization (*n* is the exponent in sp^n) of the ring carbon atom exocyclic bond (circles) and the C–CN π bond order (diamonds) in nitriles

Relative Stability

The strength of intramolecular electronic interactions can be assessed from analysis of the relative thermodynamic stability in a series of compounds. The energies for the acetylenes and nitriles relative to the respective bicyclo[2.2.2]octane derivatives **6a** and **6b** were obtained using isodesmic reactions[46]. The computational results collected in Table IX demonstrate that carborane derivatives are generally less stable than the hydrocarbon analogs. The order of stability is similar in both series of compounds and shows that the derivatives of 12-vertex *p*-carborane (**1**) are the least stable compounds, while the most stable appear to be hexatriyne (**5a**) and cubane-1,4-dinitrile (**7b**). Among the carboranes, 6-vertex cluster derivatives are generally more stable than those of 10-vertex carborane by about 4 kcal/mol, which, in turn, are more stable than those of 12-vertex cluster by about 6 kcal/mol.

The energies of isodesmic reactions reflect the differences in conjugation and electronegativity effects of the ring and the substituent. For instance, the significantly larger electron withdrawing character of the cyano group

TABLE IX
Isodesmic reactions for diacetylenes (HC≡C–A–C≡CH) and dinitriles (N≡C–A–C≡N)[a]

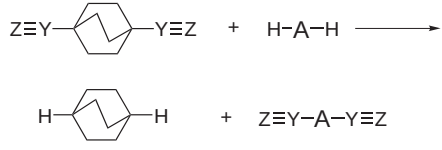

Compound	A	HC≡C–A–C≡CH **a**	N≡C–A–C≡N **b**
1	1,12-$C_2B_{10}H_{10}$	+9.2	+19.3
2	1,10-$C_2B_8H_8$	+3.5	+12.5
3	1,6-$C_2B_4H_4$	–1.8	+9.0
4	1,4-C_6H_4	–7.4	–2.0
5	1,2-C≡C	–21.6	–3.8
6	1,4-BCO	0	0
7	1,4-cubane	–9.8	–7.4

[a] The B3LYP/6-31G*//HF/6-31G* level of theory. Energy in kcal/mol.

relative to that of the acetylene substituent generally results in lower stability of the nitriles than acetylenes relative to bicyclo[2.2.2]octane derivatives. The most dramatic difference is observed for acetylene derivatives in which the strong conjugation and polar effect of the CN group destabilizes **5b** by about 18 kcal/mol relative to **5a**. The same effect is responsible for the lower stability of terephthalonitrile (**4b**) relative to 1,4-diethynylbenzene (**4a**) by about 5 kcal/mol. The relatively large decrease in the stability of the cyano carboranes relative to the acetylene analogs by about 10 kcal/mol can be attributed mainly to the unfavorable interactions between the electron deficient carborane cages and the electronegative cyano substituent. The largest effect is observed for the 6-vertex derivative (11 kcal/mol), followed by the 12-vertex (10 kcal/mol), and the least destabilizing effect of the cyano group is calculated for the 10-vertex carborane derivatives (9 kcal/mol).

The higher stability of the cubane derivatives **7** *vs* bicyclo[2.2.2]octane analogs **6** can be attributed to the more favorable hybridization of the bridgehead carbon atoms and lower hydrogen-substituent steric interactions in **7** compared with **6**.

Dediazoniation Reactions

The chemical stability of the diazo inner salts **1d**–**3d** offers another insight into the electronic interactions between boron clusters and π substituents. Computational results collected in Table X show that the heterolytic cleavage of the B–N bond and loss of N_2 has a similar endotherm for the 10-vertex, **2d** (26.2 kcal/mol) and 6-vertex, **3d** (23.7 kcal/mol) derivatives, close to the calculated (22.5 kcal/mol) and observed (23.4 kcal/mol)[47] values for benzenediazonium cation. In contrast, the 12-vertex derivative

TABLE X
Heterolytic dissociation energies for bisdiazo derivatives (N≡N–A–N≡N → N≡N–A + N≡N)[a]

Compound	A	ΔH kcal/mol	ΔG_{298} kcal/mol
1d	1,12-$B_{12}H_{10}$	23.6	12.5
2d	1,10-$B_{10}H_8$	37.5	26.2
3d	1,6-B_6H_4	35.0	23.7

[a] The B3LYP/6-31G* level of theory.

1d is predicted to be much less stable, with an endothermicity of only 12.5 kcal/mol.

Computational results are supported by experimental data. Like many benzenediazonium salts, 1,10-bis(diazo)decaborane (**2d**) is a stable compound[14] that can be sublimed below 100 °C in vacuum[14,29]. Similarly, diazotization of 1-amino-1-carbadecaborate yields an apparently persistent inner diazonium salt[48]. In contrast, diazotization of diaminododecaborate or 1-amino-1-carbadodecaborate appears to lead to an immediate loss of nitrogen and generation of highly reactive coordinatively unsaturated boron species that reacts with any nucleophile, including methylene chloride[49,50]. Although the 6-vertex analog **3d** is still experimentally unknown, the isolation of the stable B_6H_5–N≡N–B_6H_5 dianion[21] strongly suggests the relatively high stability of such a B–N≡N link in 6-vertex cluster derivatives.

A comparison of homolytic dissociation energies in series **1e**–**7e** is not as informative since the very strong polar effect of the two positively charged diazonium groups plays a very significant role in energetics of the reaction. Nevertheless, calculations show that 12-vertex carboranebisdiazonium **1e** has the lowest change of free energy among the clusters upon loss of N_2, but higher than that calculated for cubane and bicyclo[2.2.2]octane derivatives.

Spectroscopic Evidence

Electron spectroscopy provides a convenient tool for studying intramolecular electronic effects. Except for benzene, all other rings and clusters show no appreciable UV absorption above 200 nm [51–53]. This UV transparency results from relatively low lying HOMOs and large HOMO-LUMO gaps in the clusters. For instance, the calculated (B3LYP/6-31G*) HOMO energy is lower than that in benzene (–6.70 eV) by 0.64 eV for 6-vertex carborane, 0.77 eV for the 10-vertex, and 1.95 eV for 12-vertex carborane. The corresponding HOMO-LUMO energy gaps are 8.14, 7.40 and 8.60 eV for 6-, 10- and 12-vertex *p*-carboranes, respectively, which compares to the calculated 6.80 eV in benzene and 9.10 eV in acetylene. Consequently, ZINDO calculations show that the 10- and 6-vertex carboranes exhibit moderate intensity absorption bands at about 198 nm involving symmetry-allowed HOMO-LUMO (10-vertex, f = 0.35) or HOMO-LUMO+1 (6-vertex, f = 0.48) excitations with transverse transition moments. The same calculations for 12-vertex *p*-carborane show a weak band at 195 (f = 0.007) originating mainly from the HOMO-1-LUMO transition with a transverse transition moment. A significantly stronger absorption band is calcu-

lated for *p*-carborane at 167 nm. This is consistent with the observed absorption band at 200 nm (log ε = 4.6) for a 10-vertex bicarborane derivative. The analogous 12-vertex bicarborane has an absorption maximum below 195 nm [26].

Experimental data show that substitution of acetylene or cyano groups onto 12-vertex carborane has practically no effect on the absorption spectrum above 190 nm. In contrast, the acetylene and cyano derivatives of 10-vertex carborane, **2f** and **2b**, show a significant bathochromic shift relative to the parent cluster similar to that observed in the analogous benzene derivatives **4a** and **4b** [24,26]. These results are well reproduced by ZINDO calculations, which also predict a similar bathochromic shift in the derivatives of 6-vertex carborane **3**. For instance, diacetylene **2f** shows a strong transition at 233 nm [24] (calculated at 236 nm for **2a**) and nitrile **2b** exhibits a shoulder band at 219 nm (calculated at 211 nm)[24]. According to ZINDO calculations, these absorptions involve a transition from the HOMO, delocalized over the cluster and the substituent, to the LUMO, localized on the cage boron atoms, with a longitudinal transition moment (Fig. 6a). Analogous transitions in **3a** involve excitation from the HOMO to the LUMO+1 shown in Fig. 6b.

The observed significant batochromic shift in 10-vertex carboranes **2** and its absence in the 12-vertex analogs appear to be general and has been reported for other pairs of compounds **1** and **2**. Thus, the 1,10-dicyano-*closo*-

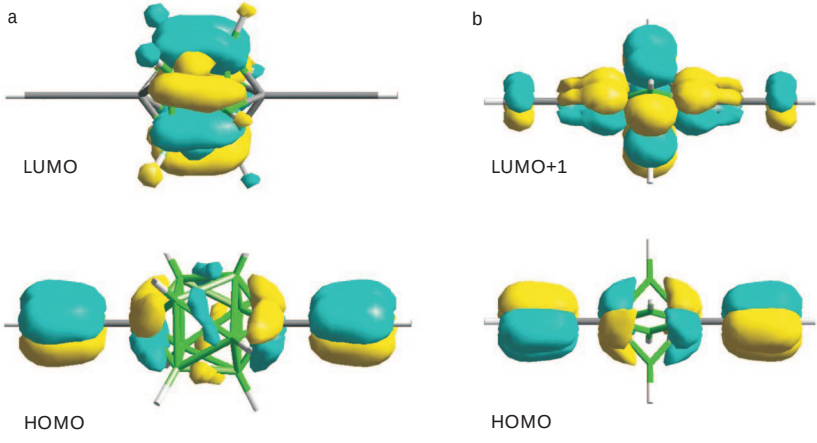

FIG. 6
A graphical representation of selected ZINDO//HF/6-31G* MOs for a 1,10-diethynyl-1,10-dicarba-*closo*-decaborane (**2a**) and b 1,6-diethynyl-1,6-dicarba-*closo*-hexaborane (**3a**)

decaborate dianion (X–Y≡Z is B–C≡N) absorbs at 250 nm (ε = 838) and 217 (ε = 54,800), while the 12-vertex analog show no maximum of absorption above 200 nm [54]. Also the dicarbonyl derivative of 10-vertex borane, **2c**, shows two intense absorption bands at 317 nm (sh, ε = 1,270) and 246 (ε = 62,000)[14].

IR spectroscopy gives insight into the bonding of functional groups. Analysis of experimental data for **1b**, **2b**, **4b**, **5b** [55], **6b** [56], and **7b** [57] in Table XI shows that the nitrile stretching frequency is similar for both 10- and 12-vertex dinitriles, **2b** and **1b**, and about 2 260 cm^{-1}. This is well reproduced by calculations, which predict very similar ν_{CN} frequencies for all three carborane nitriles. In contrast, the ν_{CN} energy in a series of cyano-*closo*-borate dianions (X–Y≡Z is B–C≡N) decreases from highest for 12-vertex dinitrile ($[1,12\text{-}B_{12}H_{10}(CN)_2]^{2-}$, 2 200 cm^{-1}), to lower for the 10-vertex analog ($[1,10\text{-}B_{10}H_8(CN)_2]^{2-}$, 2 175 cm^{-1})[54], to lowest for the 6-vertex mononitrile ($[B_6H_5CN]^{2-}$, 2149 cm^{-1})[58]. The calculated values scaled by 0.960 are 2 203, 2 182 and 2 132 cm^{-1} for the 12-, 10- and 6-vertex cyano-*closo*-borates, respectively. The same trend is observed for two carbonyl derivatives **1c** and **2c**, for which the experimental ν_{CO} are 2 210 and 2 147 cm^{-1}, respectively[20].

TABLE XI
Asymmetric stretching frequency for dinitriles (N≡C–A–C≡N)

Compound	A	ν_{CN}, cm^{-1}	
		experimental[a]	calculated[b]
1b	1,12-$C_2B_{10}H_{10}$	2 255	2 257.6
2b	1,10-$C_2B_8H_8$	2 259	2 258.6
3b	1,6-$C_2B_4H_4$	[c]	2 258.5
4b	1,4-C_6H_4	2 233	2 236.4
5b	1,2-C≡C	2 249[d]	2 240.2
6b	1,4-BCO	2 246.5[e]	2 240.9
7b	1,4-cubane	2 224[f]	2 227.3

[a] Recorded in Nujol. [b] Calculated using the B3LYP/6-31G* method and scaled by 0.9505. Overall correlation between the two sets of data is $R^2 = 0.90$ using the $y = a \cdot x$ function. [c] Not available. [d] Gas phase spectrum: ref.[55]. [e] Ref.[56]. [f] Reported for 1-(*N*-*tert*-butyl-*N*-methylcarbamoyl)-4-cyanocubane in KBr: ref.[57]

Analysis of the IR data shows no correlation between the ν_{CN} frequency and bond order, hybridization or bond length (Table V). A plausible explanation for the lack of a clear trend in the series **b** is that the ν_{CN} stretching frequency is affected by two competing effects. One effect is the bond order: the lower the bond order, the lower the wavenumber of the stretching vibration. The opposite trend is observed for polar substituents exerting inductive and field effects. This effect for a CN group in bicyclo[2.2.2]octane **6b** can be estimated at about +6 cm^{-1} (ref.[56]). Thus the polar effect of the CN group is presumably responsible for shifting the ν_{CN} frequency in **5b** to significantly higher wavenumber than that in terephthalonitrile (**4b**). Similarly, the lack of trend for ν_{CN} in the carboranenitriles can be explained by the balanced effect of decreasing bond order in the series **1b**–**3b** on one hand, and increasing the trans-cage polar effect of the CN group on the other. When the polar effects and electronegativity are dominated by the cage double negative charge in the *closo*-borate nitriles or carbonyls, the experimental ν_{CN} or ν_{CO} correlate well with the calculated bond order.

Significant differences in electronic interactions between rings and π substituents are also manifested in NMR spectra. A comparison of the effect of carboranes on the acetylene ^{13}C chemical shifts in 1-hexyne[59] with other substituents is shown in Table XII. While the effect of the 12-vertex

TABLE XII
Chemical shifts δ and chemical shift increments Δδ for selected derivatives of 1-hexyne (A–C(1)≡C(2)–C_4H_9)

A	δ		Δδ	
	C(1)	C(2)	C(1)	C(2)
H[a]	68.2	84.6	0	0
$C_2B_{10}H_{11}$[b]	75.9	83.0	+7.7	–1.6
$C_2B_8H_9$[c]	77.0	87.6	+8.8	+3.0
Me[a]	75.3	79.4	+7.1	–5.2
Ph[d]	80.6	90.6	+12.4	+6.0
MeCO[e]	81.6	91.2	+13.4	+6.6

[a] Ref.[59]. [b] Chemical shifts for 1,1′-bis(12-hept-1-ynyl-1,12-dicarba-*closo*-dodecaborane). The effect of the second cage and the chain length difference is neglected: Ref.[26]. [c] Chemical shifts for 1′-bis(10-hept-1-ynyl-1,10-dicarba-*closo*-decaborane). The effect of the second cage and the chain length difference is neglected: ref.[26]. [d] Ref.[60]. [e] Ref.[61]

carborane on acetylene is comparable to that of the methyl[59] substituent, the effect of the 10-vertex cage is more reminiscent of that of a phenyl[60] or acetyl[61] group.

CONCLUSIONS

Structural data, spectroscopic properties, chemical behavior, and electronic structure calculations are all in agreement that the degree of electronic conjugations between the cluster and triple-bonded substituent is lowest for the 12-vertex *closo*-borane and highest for the 6-vertex analogs. This is evident from the degree of "allenic distortion" of the X–Y≡Z fragment, the π bond order, and stability of the diazo compounds. For the considered series of compounds, the magnitude of electronic interactions in 6- and 10-vertex derivatives can be compared with that in benzene derivatives, while for the 12-vertex analogs the interactions are weaker, closer to those in cubane.

It appears that structural and electronic features of *closo*-boranes complement rather than duplicate those found among organic compounds. This provides an attractive alternative to control the type and degree of electronic interactions in molecular materials. Thus, 12-vertex carborane with its high symmetry and weak electronic interactions is of particular interest for designing photochemically and thermally stable liquid crystals. The more strongly interacting 6- and 10-vertex *closo*-boranes appear to be well suited for the design of NLO chromophores. The highest degree of conjugation and trans-cage interactions (*e.g.* electron transfer, spin-spin communication) is expected for the 6-vertex *closo*-borane derivatives.

Further progress in structural chemistry, spectroscopic characterization, and theoretical analysis of *closo*-borane derivatives is necessary for better understanding of the benefits and limitations of the electronic interactions offered by these fascinating inorganic ring systems.

EXPERIMENTAL

Melting points were taken in a capillary and are uncorrected. ^{1}H, ^{13}C and ^{11}B NMR spectra were obtained in $CDCl_3$ on Bruker instruments operating at 400, 100 and 128.4 MHz, respectively and referenced to the solvent (^{1}H and ^{13}C) or externally to $B(OMe)_3$ (+18.1 ppm). Chemical shifts (δ) are given in ppm, coupling constants (*J*) in Hz. IR spectra (wavenumbers in cm^{-1}) were recorded in Nujol using an ATI Mattson Genesis FT-IR. Elemental analysis was provided by Atlantic Microlab, Norcross (GE).

1,12-Dicarba-*closo*-dodecaborane-1,12-dicarbonitrile (**1b**)

A suspension of *p*-carborane-1,12-dicarboxylic acid[62] (348 mg, 1.5 mmol) and PCl_5 (660 mg, 3 mmol) in dry benzene (10 ml) was gently refluxed for 2 h, giving a homogeneous solution. Benzene and volatiles were removed in vacuum leaving a solid residue of the acid chloride. The crude chloride was dissolved in benzene (10 ml), the solution was cooled in an ice bath, and concentrated solution of ammonia (2 ml) was added. The biphasic mixture was vigorously stirred for 1 h and the resulting white suspension of the diamide **8** was filtered and dried. The crude amide and poly(trimethylsilyl phosphate) (TMSPP, 5 ml) were stirred at at 120 °C for several days, while the dinitrile was subliming into a vertical Liebig condenser fitted with a drying tube. The crystals were dissolved in CH_2Cl_2, the solution was passed through a short silica plug, and the aliquot was carefully evaporated leaving 155 mg (53% yield) of white crystals. Continued sublimation of the reaction mixture gave *ca* 90% overall yield. The dinitrile was resublimed in a sealed tube under atmospheric pressure; m.p. 155–155.5 °C. ^{13}C NMR: 60.06, 112.66. ^{11}B NMR: –13.4 (d, J_{BH} = 176). MS, *m/z*: 184–197 (max. at 194, 100%, M), 146–158 (max. at 152, 8%). IR (Nujol): 2 628, 2 255. For $C_4H_{10}B_{10}N_2$ calculated: 24.73% C, 5.19% H, 14.42% N; found: 24.99% C, 5.12% H, 14.25% N.

1,12-Bis[(trimethylsilyl)ethynyl]-1,12-dicarba-*closo*-dodecaborane[31] (**1f**)

BuLi (1.35 ml, 2.5 M in hexanes) was added dropwise to a stirred solution of *p*-carborane (231 mg, 1.60 mmol) in dry ether (5 ml) at –78 °C. The mixture was stirred at room temperature for 15 min and refluxed for 20 min. After the mixture was cooled down to –78 °C, dry CuBr (576 mg, 4.00 mmol) was added in one portion. After stirring for a further 1 h at ambient temperature a solution of 1-bromo-2-(trimethylsilyl)acetylene[63] (545 mg, 3.08 mmol) in THF (10 ml) was added. The resulting mixture was stirred at room temperature for 1 h and refluxed for 2 h. Hexane (10 ml) was added and the mixture was passed through a silica gel plug eluted with hexanes and CH_2Cl_2. The filtrate was evaporated to yield 350 mg of yellow oil which was distilled *in vacuo* collecting the fraction at 140 °C/1 torr. Gradient sublimation at 140 °C/1 torr gave the product as white crystals (55 mg, 10%); m.p. 143 °C (ref.[31] 140–141 °C). ^{1}H NMR: 0.08 (s, 18 H); 1.6–3.4 (bm, 10 H). ^{13}C NMR: –0.57, 66.01, 85.69, 100.28. ^{11}B NMR: –12.60 (d, J_{BH} = 169) (ref.[31] +11.9 ppm). MS, *m/z*: 333–339 (max. at 336, 8%), 317–325 (max. at 321, 100%).

X-Ray Crystallography

A crystal (approximate dimensions 0.15 × 0.12 × 0.01 mm for **1b** and 0.338 × 0.296 × 0.177 mm for **1f**) was placed onto the tip of a 0.1 mm diameter glass capillary and mounted on a Bruker SMART system for a data collection at 173(2) K. A preliminary set of cell constants was calculated from reflections harvested from three sets of 20 frames. These initial sets of frames were oriented such that orthogonal wedges of reciprocal space were surveyed. This produced initial orientation matrices determined from 27 and 87 reflections for **1b** and **1f**, respectively. The data collection was carried out using MoKα radiation (λ = 0.71073 Å, graphite monochromator) with a frame time of 8 s and a detector distance of 4.91 cm.

The space groups *P*-1 for **1b** and *C*2/*m* for **1f** were determined based on systematic absences and intensity statistics. A direct-methods solution was calculated which provided all non-hydrogen atoms from the E-map. Full-matrix least squares/difference Fourier cycles were performed which located hydrogen atoms and refined the structure. All non-hydrogen

atoms were refined with anisotropic displacement parameters. Hydrogen atoms of the methyl groups in **1f** were placed in ideal positions and refined as riding atoms with individual isotropic displacement parameters.

CCDC 187880 (for **1b**) and CCDC 187881 (for **1f**) contain the supplementary crystallographic data for this paper. These data can be obtained free of charge *via* ww.ccdc.cam.ac.uk/conts/retrieving.html (or from the Cambridge Crystallographic Data Centre, 12, Union Road, Cambridge, CB2 1EZ, UK; fax: +44 1223 336033; or deposit@ccdc.cam.ac.uk).

Computational Methods

Quantum-mechanical calculations were carried out using the Gaussian98 suite of programs on an SGI R8000 workstation[64]. Geometry optimizations were undertaken at the HF/6-31G* or B3LYP/6-31G* level theory using appropriate symmetry constraints and default convergence criteria. IR frequencies, zero-point vibrational energies (ZPE) and thermodynamic properties at 298 K and 1 atm were calculated using the DFT method and a scaling factor of 0.9804 (ref.[65]).

Hybridization was obtained from Natural Population Analysis using the NBO 3.1 subroutine in the Gaussian suite of programs using the *ab initio* wavefunctions. π bond orders were obtained from MNDO [66] calculations, which were performed for *ab initio*-optimized geometries using the MOPAC93 suite of programs. The parametrization of the boron atom in the AM1 method is inadequate for calculations involving boron clusters.

Electronic spectra were calculated using ZINDO (INDO/2, all electrons, no symmetry) in the Cerius2 suite of programs using HF/6-31G*-optimized geometries.

This project has been supported in part by a NSF CAREER grant (DMR-9703002).

REFERENCES AND NOTES

1. Schleyer P. v. R., Najafian K.: *Inorg. Chem.* **1998**, *37*, 3454; and references therein.
2. a) Stone A. J.: *Inorg. Chem.* **1981**, *20*, 563; b) Stone A. J., Alderton M. J.: *Inorg. Chem.* **1982**, *21*, 2297.
3. Bregadze V. I.: *Chem. Rev. (Washington, D. C.)* **1992**, *92*, 209; and references therein.
4. Preetz W., Peters G.: *Eur. J. Inorg. Chem.* **1999**, 1831; and references therein.
5. Zakharkin L. I., Kalinin V. N., Rys E. G.: *Bull. Acad. Sci. U.S.S.R., Div. Chem. Sci.* **1974**, 2543.
6. Zakharkin L. I., Kalinin V. N., Rys E. G., Kvasov B. A.: *Bull. Acad. Sci. U.S.S.R., Div. Chem.* Sci. **1972**, 458.
7. Fox M. A., MacBride J. A. H., Peace R. J., Wade K.: *J. Chem. Soc., Dalton Trans.* **1998**, 401.
8. Leites L. A., Vinogradova L. E., Kalinin V. N., Zakharkin L. I.: *Bull. Acad. Sci. U.S.S.R., Div. Chem. Sci.* **1970**, 2437.
9. Harmon K. M., Harmon A. B., Thompson B. C., Spix C. L., Coburn T. T., Ryan D. P., Susskind T. Y.: *Inorg. Chem.* **1974**, *13*, 862.
10. Grüner B., Janoušek Z., King B. T., Woodford J. N., Wang C. H., Všetečka V., Michl J.: *J. Am. Chem. Soc.* **1999**, *121*, 3122.
11. a) Murphy D. M., Mingos D. M. P., Forward J. M.: *J. Mater. Chem.* **1993**, *3*, 67; b) Murphy D. M., Mingos D. M. P., Haggitt J. L., Powell H. R., Westcott S. A., Marder T. B., Taylor N. J., Kanis D. R.: *J. Mater. Chem.* **1993**, *3*, 139.

12. Allis D. G., Spencer J. T.: *Inorg. Chem.* **2001**, *40*, 3373.
13. Bitner T. W., Wedge T. J., Hawthorne M. F., Zink J. I.: *Inorg. Chem.* **2001**, *40*, 5428.
14. Knoth W. H.: *J. Am. Chem. Soc.* **1966**, *88*, 935.
15. Harmon K. M., Harmon A. B., MacDonald A. A.: *J. Am. Chem. Soc.* **1969**, *91*, 323.
16. Kaszynski P., Huang J., Jenkins G. S., Bairamov K. A., Lipiak D.: *Mol. Cryst. Liq. Cryst. Sci. Technol., Sect. A* **1995**, *260*, 315.
17. Hawthorne M. F., Olsen F. P.: *J. Am. Chem. Soc.* **1965**, *87*, 2366.
18. Zakharkin L. I., Pisareva I. V., Sulaimankulova D. D., Antonovich V. A.: *J. Gen. Chem. U.S.S.R.* **1990**, *60*, 2453.
19. Hertler W. R., Knoth W. H., Muetterties E. L.: *Inorg. Chem.* **1965**, *4*, 288.
20. Knoth W. H., Sauer J. C., Balthis J. H., Miller H. C., Muetterties E. L.: *J. Am. Chem. Soc.* **1967**, *89*, 4842.
21. Franken A., Preetz W.: *Z. Naturforsch., B: Chem. Sci.* **1995**, *50*, 781.
22. Kaszynski P., Lipiak D. in: *Materials for Optical Limiting* (R. Crane, K. Lewis, E. V. Stryland and M. Khoshnevisan, Eds), Vol. 374, p. 341. MRS, Boston 1995.
23. Kaszynski P., Douglass A. G.: *J. Organomet. Chem.* **1999**, *581*, 28.
24. Pakhomov S., Kaszynski P., Young V. G., Jr.: *Inorg. Chem.* **2000**, *39*, 2243.
25. Kaszynski P. in: *Anisotropic Organic Materials. Approaches to Polar Order* (R. Glaser and P. Kaszynski, Eds), Vol. 798, p. 68. ACS, Washington, D. C. 2001.
26. Kaszynski P., Pakhomov S., Tesh K. F., Young V. G., Jr.: *Inorg. Chem.* **2001**, *40*, 6622.
27. Brint P., Sangchakr B., McGrath M., Spalding T. R., Suffolk R. J.: *Inorg. Chem.* **1990**, *29*, 47.
28. Fox M. A., Howard J. A. K., Moloney J. M., Wade K.: *Chem. Commun.* **1998**, 2487.
29. Whelan T., Brint P., Spalding T. R., McDonald W. S., Lloyd D. R.: *J. Chem. Soc., Dalton Trans.* **1982**, 2469.
30. Zakharkin L. I., Kovderov A. I., Olshevskaya V. A.: *Bull. Acad. Sci. U.S.S.R., Div. Chem. Sci.* **1986**, 1260.
31. Batsanov A. S., Fox M. A., Howard J. A. K., MacBride J. A. H., Wade K.: *J. Organomet. Chem.* **2000**, *610*, 20.
32. Semioshkin A. A., Inyushin S. G., Artemov V. A., Petrovskii P. V., Bregadze V. I.: *Russ. Chem. Bull.* **1998**, *47*, 1778.
33. Davidson M. G., Hibbert T. G., Howard J. A. K., Mackinnon A., Wade K.: *Chem. Commun.* **1996**, 2285.
34. Bohn R. K., Bohn M. D.: *Inorg. Chem.* **1971**, *10*, 350.
35. Hnyk D., Holub J., Hofmann M., Schleyer P. v. R., Robertson H. E., Rankin D. W. H.: *J. Chem. Soc., Dalton Trans.* **2000**, 4617.
36. Vögtle F., Frank M., Nieger M., Belser P., Zelewsky A. V., Balzani V., Barigelletti F., De Cola L., Flamigni L.: *Angew. Chem., Int. Ed. Engl.* **1993**, *32*, 1643.
37. Carballo R., Fernández-Suárez M., Muñoz L., Giguera R., Maichle-Mössmer C.: *Acta Crystallogr., Sect. C: Cryst. Struct. Commun.* **1997**, *53*, 1312.
38. Echeverria G., Punte G., Rivero B. E., Barón M.: *Acta Crystallogr., Sect. C: Cryst. Struct. Commun.* **1995**, *51*, 1020.
39. Jeffrey G. A., Rollett J. S.: *Proc. R. Soc. London* **1952**, *213*, 86.
40. Hannan R. B., Collin R. L.: *Acta Crystallogr.* **1953**, *6*, 350.
41. Ahmed N. A., Kitaigorodsky A. I., Sirota M. I.: *Acta Crystallogr., Sect. B: Struct. Crystallogr. Cryst. Chem.* **1972**, *28*, 2875.
42. Kubiak R., Janczak J.: *Acta Chem. Scand.* **1996**, *50*, 1164.

43. Kompan O. E., Antipin M. Yu., Struchkov Yu. T., Mikhailov I. E., Dushenko G. A., Olekhnovich L. P., Minkin V. I.: *J. Org. Chem. U.S.S.R.* **1985**, *21*, 1859.
44. Eaton P. E., Galoppini E., Gilardi R.: *J. Am. Chem. Soc.* **1994**, *116*, 7588.
45. Such a bond order matrix is conveniently obtained from Mulliken population analysis in the output of MOPAC calculations. Although absolute values for the π bond order estimate may not be reliable in semiempirical methods, we assume that the observed trends in series of compounds are valid.
46. Hehre W. J., Ditchfield R., Radom L., Pople J. A.: *J. Am. Chem. Soc.* **1970**, *92*, 4796.
47. Kuokkanen T.: *Acta Chem. Scand.* **1990**, *44*, 394.
48. Tsang C.-W., Yang Q., Sze E. T.-P., Mak T. C. W., Chan D. T. W., Xie Z.: *Inorg. Chem.* **2000**, *39*, 3582.
49. Pakhomov S., Douglass A. G., Kaszynski P., Young V. G., Jr.: Presented at *Boron U.S.A. VII, Pittsburgh (PA), June 2000*.
50. Nunley R., Kaszynski P.: Unpublished results.
51. Muetterties E. L., Balthis J. H., Chia Y. T., Knoth W. H., Miller H. C.: *Inorg. Chem.* **1964**, *3*, 444.
52. Thibault R. M., Hepburn D. R., Jr., Klingen T. J.: *J. Phys. Chem.* **1974**, *78*, 788.
53. Wright J. R., Klingen T. J.: *J. Inorg. Nucl. Chem.* **1970**, *32*, 2853.
54. Hertler W. R., Knoth W. H., Muetterties E. L.: *J. Am. Chem. Soc.* **1964**, *86*, 5434.
55. Khlifi M., Paillous P., Bruston P., Guillemin J. C., Bénilan Y., Daoudi A., Raulin F.: *Spectrochim. Acta, Part A* **1997**, *53*, 707.
56. Adcock W., Butt G., Kok G. B., Marriott S., Topsom R. D.: *J. Org. Chem.* **1985**, *50*, 2551.
57. Eaton P. E., Xiong Y., Zhou J. P.: *J. Org. Chem.* **1992**, *57*, 4277.
58. Preetz W., Franken A., Rath M. Z.: *Naturforsch., B: Chem. Sci.* **1993**, *48*, 598.
59. Poleschner H., Heydenreich M.: *Magn. Reson. Chem.* **1995**, *33*, 917.
60. Crisp G. T., Turner P. D., Stephens K. A.: *J. Organomet. Chem.* **1998**, *570*, 219.
61. Kalabin G. A., Proidakov A. G., Gavrilov L. D., Vereshchagin L. I.: *J. Org. Chem. U.S.S.R.* **1977**, *13*, 449.
62. Zakharkin L. I., Kalinin V. N., Podvisotskaya L. S.: *Bull. Acad. Sci. U.S.S.R., Div. Chem. Sci.* **1968**, 2532.
63. 1-Bromo-2-(trimethylsilyl)acetylene (b.p. 50 °C/1.5 torr, 66% yield) was prepared from (trimethylsilyl)acetylene according to Miller J. A., Zweifel G.: *Synthesis* **1983**, 128, in the absence of pyridine.
64. Frisch M. J., Trucks G. W., Schlegel H. B., Scuseria G. E., Robb M. A., Cheeseman J. R., Zakrzewski V. G., Montgomery J. A., Jr., Stratmann R. E., Burant J. C., Dapprich S., Millam J. M., Daniels A. D., Kudin K. N., Strain M. C., Farkas O., Tomasi J., Barone V., Cossi M., Cammi R., Mennucci B., Pomelli C., Adamo C., Clifford S., Ochterski J., Petersson G. A., Ayala P. Y., Cui Q., Morokuma K., Malick D. K., Rabuck A. D., Raghavachari K., Foresman J. B., Cioslowski J., Ortiz J. V., Baboul A. G., Stefanov B. B., Liu G., Liashenko A., Piskorz P., Komaromi I., Gomperts R., Martin R. L., Fox D. J., Keith T., Al-Laham M. A., Peng C. Y., Nanayakkara A., Gonzalez C., Challacombe M., Gill P. M. W., Johnson B., Chen W., Wong M. W., Andres J. L., Gonzalez C., Head-Gordon M., Replogle E. S., Pople J. A.: *Gaussian98, Revision A.7*. Gaussian, Inc., Pittsburgh (PA) 1998.
65. Scott A. P., Radom L.: *J. Phys. Chem.* **1996**, *100*, 16502.
66. Dewar M. J. S., McKee M. L.: *Inorg. Chem.* **1978**, *17*, 1569.